ОБЪЕДИНЕННЫЙ
ИНСТИТУТ
ЯДЕРНЫХ
ИССЛЕДОВАНИЙ

Дубна

E12-2002-297

CHEMICAL IDENTIFICATION AND PROPERTIES OF ELEMENT 112

Submitted to «Radiochimica Acta»

2002

A. B. Yakushev, Yu. Ts. Oganessian, I. Zvara, A. V. Belozerov, S. N. Dmitriev,
B. Eichler[1], S. Hübener[2], E. A. Sokol, A. Türler[3], A. V. Yeremin,
G. V. Buklanov, M. L. Chelnokov, V. I. Chepigin, V. A. Gorshkov,
A. V. Gulyaev, V. Ya. Lebedev, O. N. Malyshev, A. G. Popeko, S. Soverna[4],
Z. Szeglowski[5], S. N. Timokhin, S. P. Tretyakova, V. M. Vasko, M. G. Itkis

[1]Paul Scherrer Institute, CH-5232 Villigen PSI, Switzerland
[2]Research Center Rossendorf, 01314 Dresden, Germany
[3]Institute for Radiochemistry, Technical University of Munich, D-85748 Garching, Germany
[4]University of Bern, Department of Chemistry and Biochemistry, CH-3012 Bern, Switzerland
[5]Institute of Nuclear Physics, Krakow, Poland

Introduction

Chemical studies of element 112 (E112) are of great interest. They might test the predicted strongly pronounced "relativistic effects" in chemical properties of the element and provide an independent determination of its atomic number and decay properties. In particular, of interest is the earlier reported [2,3] isotope $^{283}112$ which can be obtained directly in the $^{238}U(^{48}Ca; 3n)$ reaction and also as the daughter of $^{287}114$ produced in the $^{242}Pu(^{48}Ca; 3n)$ reaction. According to its ground state electronic structure, E112 belongs to group 12 of the Mendeleev Periodic System (MPS), and is the nearest homologue of Hg. Then, based on classical extrapolations, E112 can form stronger bonds with surfaces of some metals, than is the bonding between E112 atoms in the hypothetic metallic phase [4]. At the same time, relativistic quantum chemistry predicts increasingly strong "relativistic effects" in the chemistry of superheavy elements (SHE) [5-9]. The calculated contraction stabilizes the spherical *s* and $p_{1/2}$ electron orbitals, which more efficiently shield the nuclear charge and thus destabilize the $p_{3/2}$- and *d*- orbitals. This may strongly influence the chemical behavior of the 7*s* and $7s7p_{1/2}$ elements, E112 and E114. They are sometimes predicted to approach noble gases in volatility and chemical inertness [8].

Many authors expected elements from112 to 118 to have unique volatility. In the 1970s, a Dubna group proposed that volatilization and similar gas-phase techniques for the chemical separation and identification of SHE 112-118 in the atomic states [4,10-15] should be used and applied them in the first experiments aimed at the search of SHE [15,16]. The adsorption behavior of SHE homologues was characterized by thermochromatography in metallic columns [17,18]. At the same time, a method of estimating adsorption energies on metals was proposed and employed to help the realization of such experiments [19,20]. Experiments confirmed the predicted rather strong interaction of the atoms of SHE homologues with the surface of transition metals. Numerous thorough tests were made with the carrier free Hg isotopes having in mind E112 [1, 21-24]. Noble metals Au, Pd and Pt were found to adsorb Hg atoms very strongly, provided that the surface was clean and above all free of oxides. Gold is the best choice for adsorbing Hg from the inert gas atmosphere at ambient temperature.

We believe that a most attractive nuclide for the first chemical identification in the SHE region is the 3-min $^{283}112$. It has a long enough half-life, and is produced in the bombardment of ^{238}U, and its formation cross section is several times higher than that for the isotopes of

E114 and E116 which are produced in the bombardment of ^{242,244}Pu and ^{248}Cm, respectively [3,25-27]. Moreover, the expected enhanced volatility of E112 makes it an ideal object for the study of its chemical behavior in the elemental state by gas-phase chemical methods. The strong interaction with suitable metallic surfaces at ambient or even lower temperatures opens up good prospects for using modern semiconductor detectors for on-line detection of volatile SHE on a one-atom-at-a time level.

The calculations and prognoses made for E112 predicted a weaker interaction with Au and a higher volatility than that of Hg [4,19,20.23,24,28,29]. Hence, one has to investigate the volatility and adsorption behavior of E112 in comparison with those of Hg and Rn. As the first stage, in our recent experiment [1] we tried to detect E112 assuming that its behavior is "Hg-like", i.e. it rather strongly adsorbs on metallic gold at ambient temperature. We observed that the simultaneously produced 49-s Hg isotope completely deposited on the surface of PIPS detectors coated with Au or Pd. We could expect to register a few SF events of E112, but we observed none. It pointed the "Hg-unlike" behavior of E112 but such was not significant from the statistical point of view. Hence, as the second stage, we had to achieve a several times higher beam dose and to detect the E112 atoms in both possible cases: 1) if E112 is a homologue of Hg and thus adsorbs on gold at ambient temperature, and 2) if the interaction with gold is weak, and E112 passes through the PIPS detectors together with Rn. For that case, a special flow-through ionization chamber was designed to register the decays.

1. Experimental

1.1. Detector for the Rn-like activity

There are two possibilities of detecting Rn-like element: to cool the semiconductor detectors to much lower temperatures so that they again retain atoms of E112, or to use a different device for direct registration of decays of E112 in gas at ambient temperature.

Thermochromatographic behavior of Rn on metallic surfaces was investigated earlier [30]. It was found that Rn atoms bind to metallic surfaces more strongly than to quartz. When searching for SHE in the ^{248}Cm + ^{48}Ca bombardments [31], radon was isolated in a gas flow and deposited onto the surface of a silicon detector cooled down to 40-60 K. Only such very low temperature ensured efficient physical (Van der Waals) adsorption of short-lived Rn isotopes on the detector. Recently, in the course of preparations to the new experiments with E112 and E114, it was found [32,33] that the temperatures of Rn deposition on clean surfaces of some transition metals (Cu, Ni, Au, Pd) were by 50 to 90 K higher than those on the

surface of an inert material (SiO_2) or oxidized metal surfaces. Taking into account that Hg is deposited on Au, Pd, and Pt even at room temperature, thermochromatography at low temperatures (with a column assembled of metal-coated α-radiation detectors) might serve for a comparative study of Hg, Rn and E112. This study is possible, in the first place, with SF-active isotope(s) such as ^{283}112. With α-active isotopes, it seems feasible only under the condition that E112 behaves similarly to Hg or at least deposits at a considerably higher temperature than Rn. Otherwise the high α-activity of Rn (plus its descendants) produced in the bombardment [34] will be collected in the low-temperature end of the column and interfere with the detection of E112.

Another possibility of detecting the noble-gas-like behavior of ^{283}112 is the measurement of SF-decaying activity in a flowing carrier gas for a few half-lives. We realized this particular variant and built a flow-through ionization chamber schematically shown in Fig. 1. We took into account the 3-min lifetime of ^{283}112 observed in physical experiments, the necessary carrier gas flow rates as well as the size of the neutron detector assembly (see below). Thus we chose a chamber of 5000 cm^3 in volume, 11 cm in diameter, and 75 cm in length. This chamber could be inserted into an assembly of neutron counters and a carrier gas hold-up time could be several minutes. The inner diameter of the cathode *1*, made from stainless steel, is 9 cm, the anode *2* is stretched along the axis of the cylindrical chamber, and the diameter of the coaxial Frish grid *3* is 2 cm. To optimize the resolution of the signals from alpha particles and fission fragments, we varied the gas composition and voltages in broad ranges. The optimal voltages were $U_{cath} = -600$ V, $U_{grid} = -470$ V, and the gas composition Ar/methane – 90:10. The current signal was taken from the anode at zero potential. Typical calibration spectra in the Ar/methane mixture are shown in Fig. 2. For the efficient detection of the "Hg-like" activity by the PIPS detectors, we had to use helium flow for its transportation from the recoil chamber to the detectors [1]. However, it was not possible to measure alpha decay and spontaneous fission in our ionization chamber with pure He or He/methane counting gas due to limited dimensions of the chamber. We found a compromise: we transported the volatile recoils and measured them in the PIPS detector setup in pure helium gas, and we added some argon and methane to the He gas at the inlet of the ionization chamber to make the ratio He/Ar/methane equal to 45:45:10. The signals coming from alpha particles had lower amplitudes with a worse energy resolution (Fig. 3a) than in the spectra measured with the optimal gas composition (Fig.2). The separation of the alpha particles and fission fragments in

the spectrum remained very good, and the shape of the fission fragment spectrum was practically unchanged, cf. Fig. 3a, b. The amplitude of fission fragment in the spectra strongly depended on specific energy losses of the detected particle. As for the particle with higher specific energy losses, the amplitude of fission fragment signal shifted to lower channels.

1.2. Experiment with element 112

The experiment was realized at the FLNR in November/December 2001. Fig. 4 shows a principal scheme of the setup. As in the first experiment in January 2000, a ~2 mg/cm^2, 20 mm in diameter $^{nat}U_3O_8$ target *2*, containing 100 μg of ^{nat}Nd was prepared onto a 2 μm HAVAR foil. It also served as a vacuum window and was supported by a thick water-cooled Cu grating *3* with an 80 % transparency. The beam energy in the half-thickness of the target layer was 234 MeV. Four similar targets were used, each of them withstood a fluence of ≈ 10^{18} particles. Hg and Rn atoms were produced in the fusion reaction ^{nat}Nd(^{48}Ca;xn) and the transfer reaction ^{238}U(^{48}Ca;Hl). In the first experiment [1], a typical beam current on the target did not exceed 0.2-0.4 pμA; it was limited by the damage to the center of the target due to the high local intensity of the beam. Now we used a wobbler device *5*, which distributed the beam current uniformly over the target; it allowed us to double the mean beam current on the target. After 22.5 days of the bombardment with ^{48}Ca ions (E_{init} = 262 MeV, I = 0.6 pμA), an integral beam dose of 2.8x10^{18} was accumulated (taking into account the transparency of the supporting grate).

The recoils were thermalized in pure helium at the pressure slightly above atmospheric (the target chamber *1* volume was 45 cm^3) and transported through a 25 m long, 2 mm i.d. PTFE capillary (80 cm^3 in volume) to the detectors situated behind a concrete wall, which served as a shield against gamma radiation and neutrons from the cyclotron. The first detector assembly *6*, an upgraded version of that used earlier [1], was a disk chamber with 8 PIPS sandwiches; all the 16 PIPSs, with the working area of 18x18 mm^2 each, were covered with 30 μg/cm^2 Au. The gap between the "top" and "bottom" detectors was 1 mm; cf. Fig. 5a. The gas exiting the chamber *6* was mixed with appropriate quantities of Ar and methane. Then it passed through an aerosol filter into the ionization chamber *7*. Both detection chambers were positioned inside a 1 m long assembly of 126 ^{3}He-filled counters *8* (in a moderator) to register prompt fission neutrons as an additional indication of fission events. The pulses from the PIPSs and ionization chamber in the energy range of fission fragments triggered measurement of prompt fission neutrons, which lasted 128 μs thus overlapping more than 99% of the

lifetime distribution of fission neutrons in the neutron detector [35]. Simultaneously with the amplitude, the time coordinates of all the pulses from the PIPS detectors, as well from the ionization chamber were measured with a time resolution of 1 μs. Now that the data acquisition system had been upgraded we could search for the $\alpha - \alpha$, $\alpha - SF$ and $SF - n$ correlations in the course of the on-line analysis.

2. Results and Discussion

2.1. Observation of element 112

Three flow rates of He gas (250 cm^3/min, 500 cm^3/min and 1000 cm^3/min) were used during the bombardment to overlap a considerable uncertainty in the reported [2] half-life of $^{283}112$, at the production of which we aimed. The times of complete displacement of the He/Ar/methane gas in the ionization chamber were 9, 4.5, and 2.3 min, respectively (the flow rate was 2.2 times higher than that of He). When the time is 9 min, at least 80% of the 3-min gaseous activity must decay in the chamber. Table 1 summarizes the experimental conditions. The behavior of Hg and Rn atoms in the PIPS detector assembly was traced by registering the α-decays of ^{185}Hg ($T_{1/2}$ = 49 s) and ^{220}Rn ($T_{1/2}$ = 55 s). We did not observe any significant difference in the transportation time of ^{185}Hg and ^{220}Rn through the PTFE capillary. However, when Hg and Rn reached the Au-coated PIPS detectors, at a He flow rate of 500 cm^3/min., 95% of the 49-s ^{185}Hg was adsorbed already in the first sandwich, and 99% - was deposited when the flow rate was 250 cm^3/min. In contrast to this, only a minute part of the Rn activity decayed within the PIPS detector assembly and was distributed practically evenly over all the 8 pairs of the PIPSs (Fig.6). In our previous experiments with Hg and E112 we learned that non-volatile elements produced in nuclear reactions were retained in the recoil chamber and in the first centimeters of the PTFE capillary. Volatile metals (Hg and At) and non-metals (F, Cl, Br) adsorbed strongly on the Au coating of silicon detectors. Hence, only chemically inert very volatile species could reach the exit of the PIPS detector setup. It was confirmed by measurements of the long-lived activities after the present experiment.

We measured the distribution of long-lived gamma activities and alpha emitters in the recoil chamber, PTFE capillary, and on the PIPS detectors after a long run. At the detector entrance, in the spectra we only found scarce counts (at the detection limit) from the non-volatile species (Pd, Rh, Ru and actinides, originating in the target and target backing). The

factor of purification of gaseous elements evaluated from the detection limits in the gamma spectra was $\geq 10^4$. Measurements of long-lived alpha emitters in the recoil chamber and on the PIPSs raised this factor to $5 \cdot 10^5$. Under the experimental conditions, no known volatile species of heavy actinides or light transactinides could be formed and if some non-volatile species could reach the detectors, it could only happen due to possible aerosol transportation. But the aerosol filter installed between the PIPS detector assembly and the ionization chamber was bound to further increase the 10^4 factor of chemical purification from non-volatile products.

We also measured a long-lived SF activity accumulated in the target, on the walls of the recoil chamber and inside the PTFE capillary using the solid-state track detector technique. For one of the four used targets, the measurements were made in a wide range of times: the first one was made one hour after the irradiation and the last one - 10 months after it (Table 3). The larger part of this activity decays with a half-life of ≈2 months; most probably, it is ^{254}Cf. Then the smaller part can be attributed to the longer-lived ^{252}Cf. Evidently, no considerable activity with an hours' half-life was produced. If so, the production cross sections for ^{252}Cf and ^{254}Cf in the ^{238}U + ^{48}Ca bombardment are 500nb and 3nb, respectively. As much as 85% of the produced long-lived SF activity remained in the 2mg/cm^2-thick uranium target (cf. Table 3). The achieved purification factor is far in excess of what was needed to completely remove the non-volatile SF activity from the gas.

During the whole time of the bombardment, there came no signal with an energy higher than 12 MeV from the PIPS detectors, i.e. no SF event happened. As for the ionization chamber, we regarded as SF events only the signals registered in the 700-th channel and upwards (cf. Fig. 3b) in coincidence with neutrons. During two weeks before and twelve weeks after the experiment, we measured a possible SF background of the ionization chamber. Within 100 days of measurements, a total of 4 signals in the fission fragment range of the spectra was observed. Hence, the expected background rate for the duration of our experiment was ≈ 1 SF event. The source of this extremely low background is difficult to establish conclusively.

In the experiment, there occurred eight SF events in the ionization chamber (Table 2). So these events could be attributed only to a very volatile and chemically inert SF activity. All the signals came with amplitudes close to that of a single fission fragment (see Fig. 3b), so the decays seem to have taken place mostly on or near the surface. From the data, the shortest 68% and 95% confidence intervals [36] for the mean "counting rate" of the "net" events are $7^{+3.2}_{-2.5}$ and $7^{+7}_{-4.4}$, respectively. Thus, the non-zero number of the net counts is highly

significant statistically. The data of Tables 1 and 4 demonstrate that the lifetime of the observed SF activity must be longer than 1 minute or so. This is consistent with the value of the lifetime measured previously [2,3] for ^{283}112. Most probably, we have observed this activity. The measurement of prompt neutrons could not be used for the evaluation of their average number because of low statistics and insufficient knowledge of the coordinates of each decay event. From the above limits for the net counts assuming an effective target thickness of 1 mg/cm^2 ^{238}U and an overall procedure efficiency of 50% we evaluated the effective production cross section of ^{283}112 in the reaction ^{238}U + ^{48}Ca as $\sigma = 2^{+0.9}_{-0.7}$ pb and $2^{+2.0}_{-1.2}$ pb for the shortest 68% and 95% confidence intervals, respectively.

2.3. Chemical characterization of element 112

The distributions of volatile nuclides at various flow rates and the retention times measured for Hg and Rn isotopes and evaluated for E112 as inert gas are summarized in Table 4. The retention time was calculated proceeding from the distribution and half-life for each nuclide. Then, using the model of mobile adsorption for the description of migration velocity of species in chromatographic column and a Monte Carlo simulation [37,38], we evaluated the adsorption enthalpies of Rn and E112 on the gold surface of PIPSs. For Rn it is $-\Delta H_{ads}(\mathrm{Rn}) \approx$ 36 kJ/mol, which is in good agreement with the value obtained by vacuum thermochromatography [32]. In the case of the 3-min ^{283}112, from the estimated upper limit of the retention time we calculated the upper limit to be $-\Delta H_{ads}(112) \leq 60$ kJ/mol. The adsorption enthalpy of Hg is much higher (114 kJ/mol; see Ref. [24]). The quantity $-\Delta H_{ads}$ can be considered as the sum of the "net" desorption enthalpy and the standard sublimation enthalpy of the adsorbate [29]. One cannot measure both constituent enthalpies separately in one experiment. Meanwhile, the limit $-\Delta H_{ads} \leq 60$ kJ/mol is less than the sublimation Hg enthalpy of 62 kJ/mol. Hence, the E112 bulk must be more volatile than Hg.

Thus, in the atmosphere of an inert gas in contact with PTFE and stainless steel, the atoms of E112 behave in accordance with the predicted enhanced volatility of the element. In addition, they do not form strong metal-metal bonds when hitting the Au surface. In other words, E112 behaves more like the noble gas Rn rather than Hg. Such marked difference in the chemical properties of the transactinide and its nearest homologue in the MPS was demonstrated for the first time. Undoubtedly, the next step is a quantitative comparative study of physical-chemical properties of Hg, Rn and E112.

Table 1. Experimental conditions

Target /Beam energy, MeV	Max/Mean intensity, pμA	Duration, days	Beam dose, particles x10^{-18}/ Number of events	He/Ar/methane flow rates, cm^3/min
^{nat}U (2 mg/cm^2) + ^{142}Nd (100 μg/cm^2) on 2 μm HAVAR E_{Ca} = 234 MeV in the half-thickness of the target	0.6 / 0.3	10.5	1.25 / 3	250/250/50
	0.6 / 0.4	9	1.25 / 3	500/500/100
	0.6 / 0.3	3	0.3/ 2	1000/1000/100

Table 2. SF events observed in the ionization chamber

Event No. Date / Time	Energy, channel number (cf. Fig.3)	Number of correlated neutron counts	Time distribution of neutrons,	Gas flow rate He/Ar/methane, cm^3/min
1. 14.11/00:39	1248	3	0*, 8, 10	250/250/50
2. 25.11/18:48	923	3	0*, 10.5, 122	500/500/100
3. 27.11/16:39	933	1	24.5	250/250/50
4. 30.11/03:59	1308	1	12	250/250/50
5. 02.12/04:29	936	1	3.5	500/500/100
6. 07.12/05:40	967	1	80	500/500/100
7. 07.12/20:47	962	2	1, 6.5	1000/1000/100
8. 08.12/12:10	1396	1	0*	1000/1000/100

* - time is less than 1 μs.

Table 3. Distribution of the long-lived SF activity

Time after the bombardment	SF activity, counts/day			
	2 mg/cm^2 - ^{238}U target	2 mg/cm^2 - ^{238}U target beam dose - 10^{18}	Recoil chamber	PTFE capillary (first meter)
Before the bombardment	4	-	-	-
1 hour	-	150	-	-
1 week	-	140	-	-
1month	-	120	11	10
3 months	-	-	-	6
10 months	-	11	-	-

Table 4. Distribution and retention time of volatile nuclides

Gas flow rate, cm^3/min	Nuclide	Activity, %*) / Retention time, min			
		Recoil chamber	PTFE capillary	PIPS detectors	Ionization chamber
250/250/50	^{220}Rn (55 s)	- / 0.2	40 / 0.7	0.8 / 0.01	~ 60 / 10.3
	^{185}Hg (49 s)	16 / 0.2	45 / 0.7	39 / ≥ 24	-
	^{283}112 **)	**4.5 / 0.2**	**15 / 0.7**	**<20 / ≤ 1**	**> 60 / 11.7**
500/500/100	^{220}Rn (55 s)	- / 0.1	23.6 / 0.35	0.4 / 0.005	~75 / 5.1
	^{185}Hg (49 s)	8.3 / 0.1	26 / 0.35	65.7 / ≥ 12	-
	^{283}112 **)	2.3 / 0.1	8 / 0.35	<11 / ≤ 0.5	> 60 / 5.85
1000/1000/100	^{220}Rn (55 s)	- / 0.05	12.3 / 0.17	0.2 / 0.0025	~80 / 2.6
	^{185}Hg (49 s)	4.3 / 0.05	14 / 017	81 / ≥ 6	
	^{283}112 **)	**1.2 / 0.05**	**4 / 0.17**	**< 6 / ≤ 0.25**	**> 43 / 2.9**

*) Percent of decays which occurred within this part. The 100% yield was measured in separate bombardments: for Hg - with a catcher foil behind the target, for Rn – with a charcoal filter at the exit from the recoil chamber.

**) estimated with $T_{1/2}$ = 3 min.

Acknowledgements

This work has been done with the support of Grants of Plenipotentiaries of Czech Republic and Republic of Poland in the JINR (1999–2001) and the RFBR Project #02-02-16116. We would like to thank the staff of the U-400 cyclotron and of the ion source group for providing the intense ^{48}Ca ion beam.

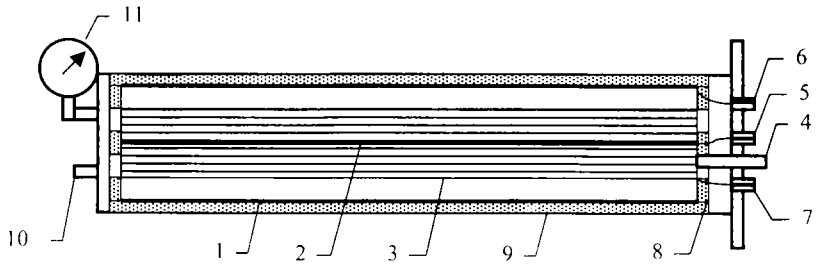

Figure 1. Schematic view of the ionization chamber:

1- cathode; 2- anode; 3- Frish grid; 4- gas inlet; 5,6,7- connectors; 8- insulation; 9- housing; 10- gas outlet; 11- manometer.

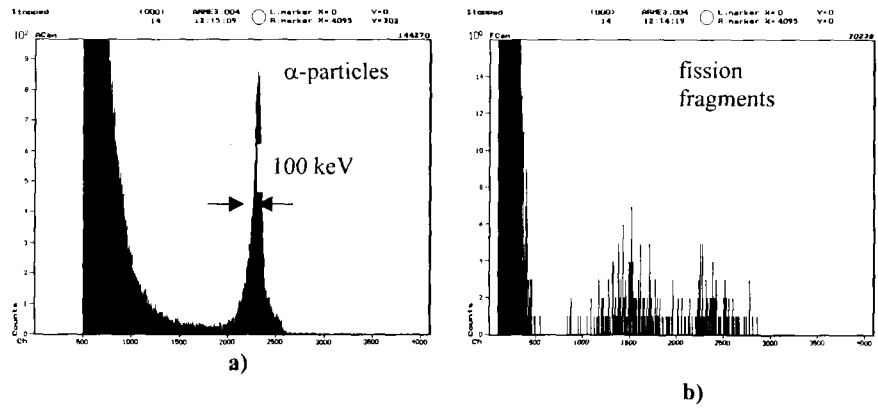

Figure 2. Ionization chamber spectra measured in the Ar/methane (90:10) mixture:

a) alpha particles from a thin ^{235}U source;

b) fission fragments from the thermal neutron induced fission in the source.

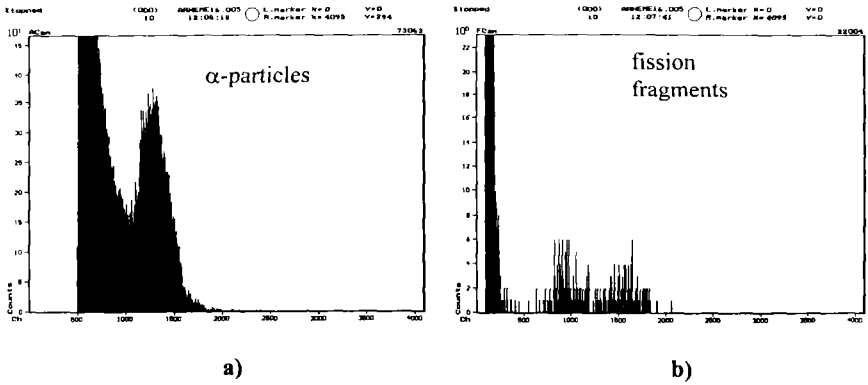

Figure 3. *Ionization* chamber spectra measured in the He/Ar/methane (45:45:10) *mixture:*

a) alpha particles from a ^{235}U thin source;

b) fission fragments from the thermal neutron induced fission in the source.

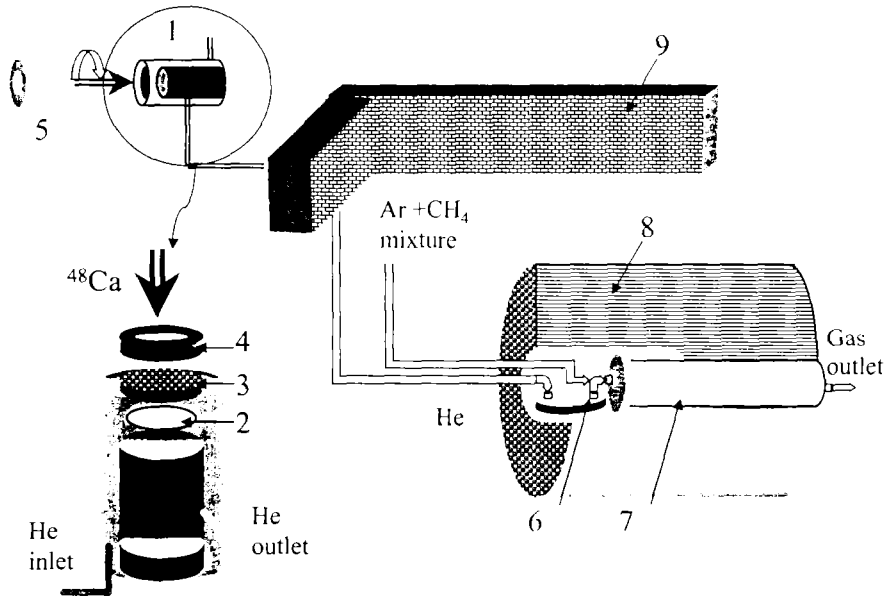

Figure 4. Schematic view of the experimental setup:

1 – recoil chamber; 2 – ^{238}U target; 3 – Cu grating; 4 – Cu collimator;
5 – wobbler device; 6 – chamber with 8 pairs of PIPS detectors;
7 – ionization chamber; 8 - assembly of 126 ^{3}He neutron counters; 9 – biological shielding wall.

a) b)

Figure 5. View of the open PIPS detector assembly* (a) and ionization chamber (b).

* Only 8 bottom detectors mounted in the PTFE disks are shown. The top detectors, gas inlet and outlet as well as covers are removed.

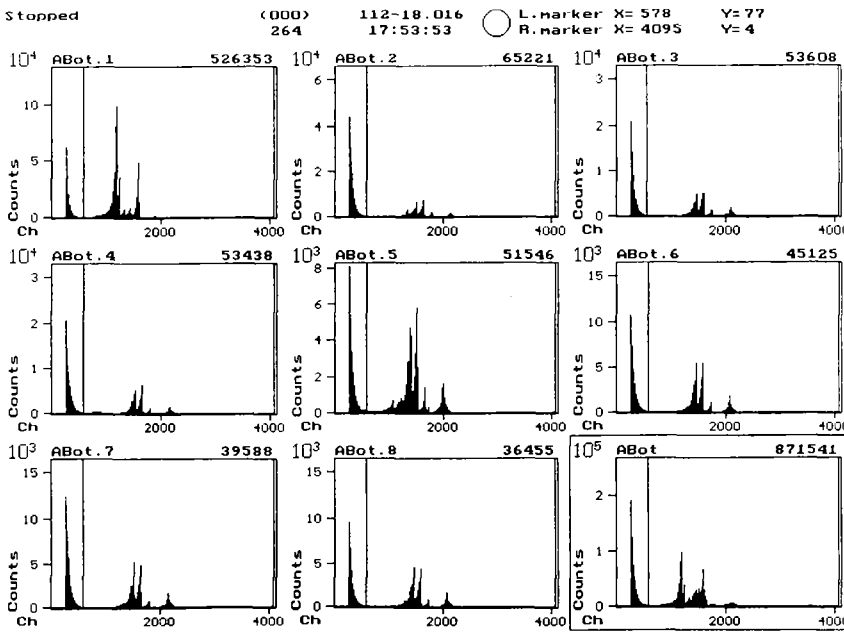

Figure 6. Alpha spectra from 8 bottom PIPS detectors:

ABot1 – ABot8: single alpha spectra from bottom detectors 1 - 8, Abot: the sum spectrum. The numbers in the right-hand upper corner of each spectrum correspond to alpha counts between markers. The main alpha activity coming from ^{185}Hg is deposited on detector 1. Rn and its descendants are distributed practically evenly.

References

1. Yakushev, A. B.; Buklanov, G. V.; Chelnokov, M. L.; Chepigin, V. I.; Dmitriev, S. N.; Gorshkov, V. A.; Hübener, S.; Lebedev, V. Ya.; Malyshev, O. N.; Oganessian, Yu. Ts.; Popeko, A. G.; Sokol, E. A.; Timokhin, S. N.; Türler, A.; Vasko, V. M.; Yeremin, A. V.; Zvara, I. *Radiochim. Acta* **89**, 743-745 (2001).
2. Oganessian, Yu. Ts.; Yeremin, A. V; Gulbekian, G. G.; Bogomolov, S. L.; Chepigin, V. I.; Gikal, B. N.; Gorshkov, V. A.; Itkis, M. G.; Kabachenko, A. P.; Kutner, V. B.; Lavrentev, A. Yu.; Malyshev, O. N.; Popeko, A. G.; Roac, J.; Sagaidak, R. N.; Hofmann, S.; Münzenberg, G.; Veselsky, M.; Saro, S.; Iwasa, N.; Morita, K. *Eur. Phys. J. A* **5**, 63 (1999).
3. Oganessian, Yu. Ts.; Yeremin, A. V; Popeko, A. G.; Bogomolov, S. L.; Buklanov, G. V.; Chelnokov, M. L.; Chepigin, V. I.; Gikal, B. N.; Gorshkov, V. A.; Gulbekian, G. G.; Itkis, M. G.; Kabachenko, A. P.; Lavrentev, A. Yu.; Malyshev, O. N.; Roac, J.; Sagaidak, R. N.; Hofmann, S.; Veselsky, M.; Saro, S.; Giardina, G.; Morita, K. *Nature* **400**, 242 (1999).
4. Eichler, B. *Kernenergie* **19**, 307 (1976).
5. Fricke, B; Waber, J.T. *Act. Rev.* **1**, 433 (1971).
6. Pitzer, K. J. *Chem. Phys.* **63**, 1032 (1975).
7. Pyykkö, P. *Chem. Rev.* **88**, 563 (1988).
8. Schwerdtfeger, P.; Seth, M. *In Encyclopedia of Computional Chemistry*; Willey: New York, Vol. 4, 2480-2499 (1998).
9. Pershina, V. G. *Chem. Rev.* **96**, 1977 (1999).
10. Eichler, B. *JINR Reprint P12-7767* (in Russian), Dubna (1974).
11. Eichler, B. *JINR Reprint P12-6662* (in Russian), Dubna (1972).
12. Eichler, B. *J. Inorg. Nucl. Chem.* **35**, 4001 (1973).
13. Zvara, I., Eichler, B., Belov, V. Z., Zvarova, T. S., Korotkin, Yu. S., Shalaevski, M. R., Shchegolev, V. A., Hussonois, M. *Radiokhimiya* (in Russian) **15**, 720 (1974).
14. Reetz, T., Eichler, B., Gäggeler, H. W., Zvara, I. *Radiochim. Acta* **24**, 69 (1977).
15. Reetz, T, Eichler B., Brichertseifer, H., Zhuikov, B. L., Belov, V. Z., Zvara, I. *Radiokhimiya* (in Russian) **6**, 877 (1979).
16. Oganessian, Yu. Ts., Bruchertseifer, H., Buklanov, G. V., Chepigin, V. I., Choi Val Sek, Eichler, B., Gavrilov, K. A., Gäggeler, H. W., Korotkin, Yu. S., Orlova,

O. A., Reetz,, T., Seidel, W., Ter-Akopian, G. M., Tretjakova, S. P., Zvara, I. *Nuclear Phys.* **A294**, 213 (1978).

17. Eichler, B., Reetz, T., Domanov, V. P. *JINR Reprint P12-10047* (in Russian), Dubna (1976).
18. Eichler, B., Reetz, T. *Kernenergie*, **25**, 218 (1981).
19. Rossbach, H., Eichler, B. *Reprint ZfK-527*, Rossendorf (1984) ISSN 0138 2950.
20. Eichler, B., Rossbach, H. *Radiochim. Acta* **33**, 121 (1983).
21. Eichler, B., T., Domanov, V. P. *JINR Reprint P12-7928* (in Russian), Dubna (1974).
22. Eichler, B., Kim Son Chun. *JINR Reprint P12-83-206* (in Russian), Dubna (1983).
23. Eichler, B., Hübener, S., Zhuikov, B. L., Rossbach, H. *JINR Reprint P12-81-717* (in Russian), Dubna (1981).
24. Soverna, S., Düllmann, Ch., Gäggeler, H. W., Türler, A., Eichler, B., Piguet, D., Tobler, L., Zhi, Q. *PSI Annual Report 2001*, PSI Villigen (2002).
25. Oganessian, Yu. Ts.; Utyonkov, V. K.; Lobanov, Yu. V.; Abdullin, F. Sh.; Polyakov, A. N.; Shirokovsky, I. V.; Tsyganov, Yu. S.; Gulbekian, G. G.; Bogomolov, S. L.; Gikal, B. N.; Mezenttsev, A. N.; Iliev, S.; Subbotin, V. G.; Sukhov, A. M.; Buklanov, G.V.; Subotic, K.; Itkis, M. G.; Moody, K. J.; Wild, J. F.; Stoyer, N. J.; Stoyer, M. A.; Lougheed, R. W. *Phys. Rev. Lett.* **83**, 3154 (1999).
26. Oganessian, Yu. Ts.; Utyonkov, V. K.; Lobanov, Yu. V.; Abdullin, F. Sh.; Polyakov, A. N.; Shirokovsky, I. V.; Tsyganov, Yu. S.; Gulbekian, G. G.; Bogomolov, S. L.; Gikal, B. N.; Mezenttsev, A. N.; Iliev, S.; Subbotin, V. G.; Sukhov, A. M.; Ivanov, O. V.; Buklanov, G.V.; Subotic, K.; Itkis, M. G. *Phys. Rev. C* **62**, 041604(R) (2000).
27. Oganessian, Yu. Ts.; Utyonkov, V. K.; Lobanov, Yu. V.; Abdullin, F. Sh.; Polyakov, A. N.; Shirokovsky, I. V.; Tsyganov, Yu. S.; Gulbekian, G. G.; Bogomolov, S. L.; Gikal, B. N.; Mezenttsev, A. N.; Iliev, S.; Subbotin, V. G.; Sukhov, A. M.; Buklanov, G.V.; Subotic, K.; Itkis, M. G.; Moody, K. J.; Wild, J. F.; Stoyer, N. J.; Stoyer, M. A.; Lougheed, R. W.; Laue, C. A.; Karelin, Ye. A.; Tatarinov, A. N. *Phys. Rev C* **63**, 011301(R) (2000).
28. Eichler, B., Eichler, R., Gäggeler, H. W. PSI *Annual Report 2000,* PSI Villigen (2001).
29. Eichler, B. *PSI Reprint 00-09*, PSI Villigen (2000) ISSN 1019 0643.

30. Eichler, B., Kim Son Chun. *Isotopenpraxis* **5**, 180 (1985).

31. Gäggeler, H. W.; Brüchle, W.; Brügger, M.; Schädel, M.; Sümmerer, K.; Wirth, G.; Kratz, J. V.; Lerch, M.; Blaich, T.; Herrmann, G.; Hildebrand, N.; Trautmann, N.; Lee, D.; Moody, K. J.; Gregorich, K. E.; Welch, R. B.; Seaborg, G. T.; Hoffman, D. C.; Daniels, W. R.; Fowler, M. M.; von Gunten, H. R. *Phys. Rev. C* **33**, 33 (1986).

32. Eichler, R.; Schädel, M. *J. Phys. Chem. B* **106**, 5413-5420 (2002).

33. Eichler, R., Eichler, B. *PSI Annual Report 2000*, PSI Villigen (2001).

34. Dressler, R. *In* Proceedings *of Workshop ChemSep'02*, GSI, Darmstadt (2002), http://www.gsi.de/chemsep/.

35. Sokol, E.A. et. al. *Nucl. Instr. Meth.* **A400**, 96 (1997).

36. Helene, O. *Nucl. Instr. Meth.* **228**, 120-128 (1984).

37. Eichler, B., Zvara, I. *Radiochim. Acta* **30**, 233-238 (1982).

38. Zvara, I. *Radiochim. Acta* **38**, 95-101 (1985).

Received on December 29, 2002.